# An Ultra-light and Flexible sEMG Active Probe for Patch-like Muscle Activity Monitoring

# An Ultra-light and Flexible sEMG Active Probe for Patch-like Muscle Activity Monitoring

Letizia Cantore, Fabio Rossi, Andrea Mongardi, Danilo Demarchi
Department of Electronics and Telecommunications, Politecnico di Torino, Turin, Italy, Email: fabio.rossi@polito.it

***Abstract*—Surface ElectroMyoGraphy (sEMG) constitutes a valid tool for monitoring muscle activity in sports, rehabilitation, control of Human-Machine Interfaces (HMIs), and tele-monitoring. To extend its applicability beyond clinical settings, the wearability of acquisition systems is a key factor, allowing for reduced discomfort during use, acquiring signals without hindering movement, and reducing the risk of detachment during the acquisition. This paper proposes a flexible, lightweight (0.81 g), and extremely compact active probe, measuring 30 mm x 10 mm x 3 mm, produced using rigid-flex PCB technology. The experimental tests, conducted on five subjects, each one performing six dynamic movements, show that the developed probe is capable of acquiring good quality sEMG signals, with a median Signal-to-Noise Ratio (SNR) of 10.9 dB. Additionally, the minimal power consumption of the active probe, amounting only to 0.732 mW, makes the probe suitable for battery-powered applications, e.g., activities of daily living long-term recordings.**

***Index Terms*—Surface Electromyography, Active Electrodes, Flexible Electronics, Wearable Sensors, Muscle Monitoring**

## I. INTRODUCTION

Surface ElectroMyoGraphy (sEMG) is a non-invasive technique used to capture electrical signals originating from the depolarization of muscle fiber membranes by placing electrodes on the skin [1], [2]. It serves as a particularly valuable tool in various research and clinical fields, such as rehabilitation [3]–[11], control of Human-Machine Interfaces (HMIs) [12], [13], neuro-prosthetics activation and feedback [14], [15], and quantitative assessment, like sports performance evaluation [16]–[18] and gait and postural tracking, in the fields of ergonomics and tele-monitoring [19]–[21].

A critical aspect of using sEMG recording devices for muscle activity monitoring is their wearability. Indeed, recent research [22] has focused on alternatives to disposable silver/silver chloride (Ag/AgCl) wet-gel electrodes due to their size, the need for bulky shielded cables and rigid electrode holders, and the potential for skin irritation, in addition to dehydration over time resulting in signal degradation. Capacitive and surface direct-contact dry electrodes offer a viable alternative to traditional ones, eliminating the need for gel and enabling reusability. Dry-contact electrodes consist of conductive materials, such as biocompatible metals, carbon, or conductive polymers, and rely on skin sweat and moisture as the electrolyte, which reduces contact impedance over time [22], [23]. Capacitive electrodes use a conductive plate covered by a dielectric material to detect electrical displacement currents through capacitive coupling, providing greater comfort, reduced allergy risk, and no need for skin preparation. However, they have higher skin-electrode impedance

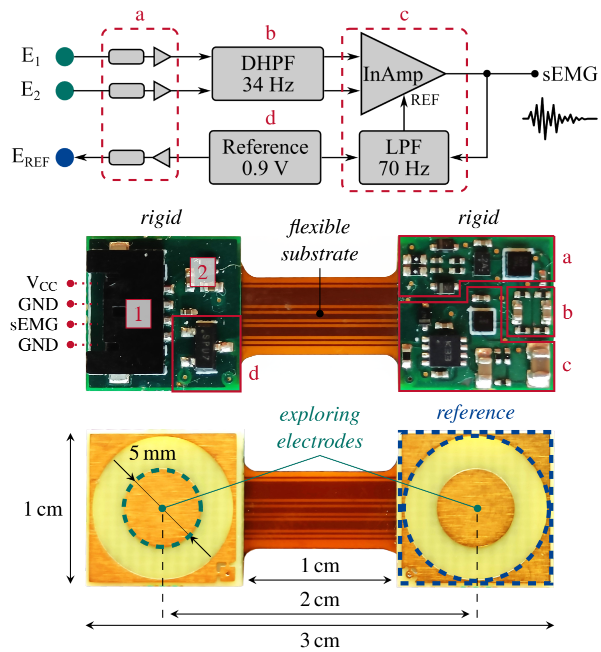


Fig. 1. The sEMG active probe prototype (bottom) and its functional components (top). The signal is decoupled (a), differential high-pass filtered to get rid of movement artifacts (b), and then amplified (c). A DC offset (d) is provided to both the reference electrode and the INA REF input.

and generally higher manufacturing costs [22], [23]. In both cases, it is advisable to implement bio-signal active probe strategies to reduce sensitivity to noise and motion artifacts, i.e., integrating operational amplifiers directly on the top of the biopotential recording electrode. This solution increases the input resistance seen by the electrodes, reducing signal attenuation, and decreases the output resistance seen by the acquisition system, minimizing noise. As a result, active probes are less susceptible to electromagnetic interference and motion artifacts, and allow the use of longer cables without signal degradation [24].

This paper presents a custom semi-flexible active probe (Fig. 1), designed focusing on minimizing power consumption and device area while maintaining adequate mechanical strength and suitable signal quality for muscle activity monitoring. The central flexible segment, together with the overall thinness (i.e., 3 mm) of the PCB, make the proposed probe perfect to be patched for long-term wearable applications, also involving powerful dynamic exercises.

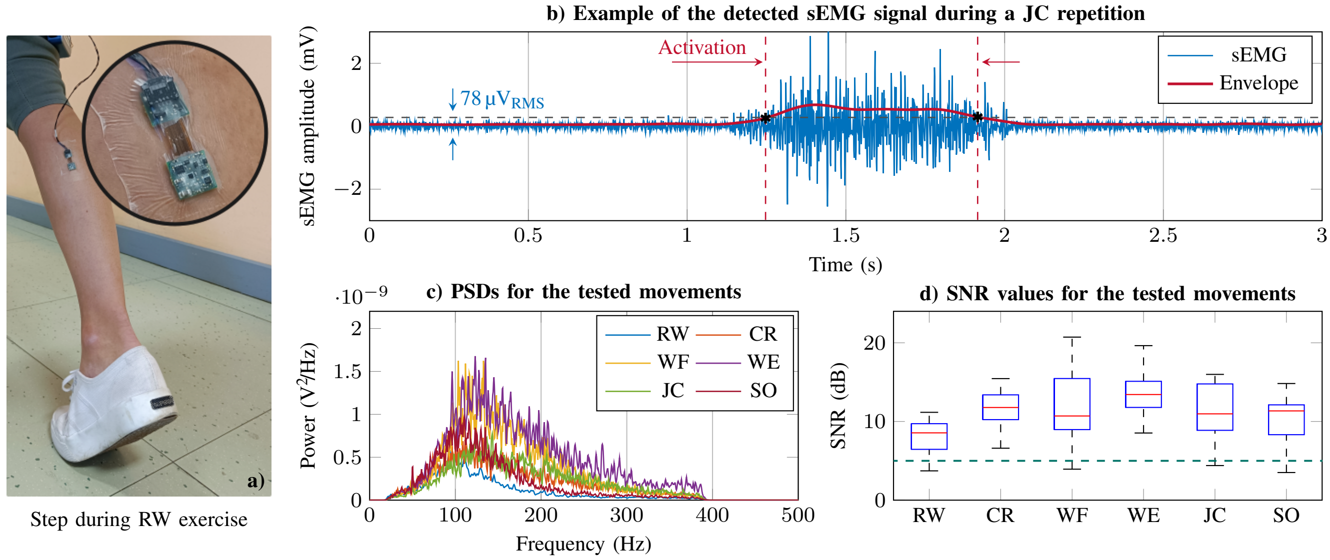


Fig. 2. **a)** shows a photo to demonstrate how the active probe can be worn, here sensing the activity of the *gastrocnemius medialis* muscle during gait; **b)** reports an example of the recorded sEMG at the *temporalis* site, displaying both rest and contraction muscular phases; **c)** represents the PSDs of our frequency analysis, demonstrating how the active probe correctly detect typical sEMG frequencies, and **d)** summarizes the SNR results for all tested movements.

## II. sEMG Active Probe Design and Prototype

The proposed active probe consists of two square rigid regions (10 mm x 10 mm), with a four-layer stack-up, connected by a flexible bridge (5 mm x 10 mm) made of polyimide.

The bottom side of the rigid regions includes an exploring electrode and a reference electrode, both gold-plated to be dry, bio-compatible, and reusable. The electrode configuration was optimized for differential signal acquisition, balancing signal quality and active probe size. An Inter-Electrode Distance (IED) of 20 mm was chosen based on the SENIAM guidelines [25]. The exploring electrodes have a diameter of 5 mm, which reduces crosstalk from nearby muscles and minimizes the low-pass filtering effect inherent to the sensing area [26]. The reference electrode was designed to surround the exploring electrodes at a distance of 2 mm, thus not interfering with it but still maintaining its electrical continuity.

On the top side of the rigid regions, all the electronic components have been meticulously positioned to fit the 200 mm$^2$ area. Looking at the central section of Fig. 1, the top layer includes a Pico-Lock connector (1) to interface the active probe with an external system, a low drop-out voltage regulator (2) to provide a stable 1.8 V power supply, and the AFE (a–d) for signal conditioning. In particular, the AFE chain is based on the design previously described in [27], from which the following stages were here re-implemented for the active probe design:

a) electrodes protection and impedance decoupling;
b) Differential High-Pass Filter (DHPF), with 34 Hz cutoff frequency, to attenuate motion artifacts;
c) Instrumentation Amplifier (InAmp), further stabilized by a 70 Hz Low-Pass Filter (LPF) as negative feedback on its reference, to obtain the amplified (200 V/V) differential sEMG signal;
d) the 0.9 V reference generator used both to impose the skin potential and to refer the InAmp output to the middle dynamic.

In this way, the resulting sEMG signal, whose example representation is reported in Fig. 2-b, is sufficiently robust to be wired-transmitted to a second unit, where optional AFE stages could be implemented to further enhance signal quality, e.g., adding the programmable gain multiplier or the 400 Hz LPF of our previous design [27].

To complete the design, the flexible substrate provides both power supply and signal paths between the two rigid regions, and guarantees good adaptation to skin and muscle anatomy thanks to the bending and torquing capability of the polyimide layer (Fig. 2-a).

## III. Validation Tests and Results

The performance of the developed active probe has been evaluated by carrying out two tests: the assessment of the sEMG signal quality and the power consumption analysis.

Five healthy subjects, aged between 25 and 30 years old, were recruited to test the actual usability of the active probes. Each subject was asked to perform 10 dynamic contractions of 6 common movements. The active probe was attached to the skin with a bio-compatible adhesive tape, above one of the primarily activated muscles for each exercise, according to the SENIAM guidelines [25], [33]. The active probe was then connected to the NI USB-6003 data acquisition (DAQ) board, linked to a computer. The movements performed, with the relative muscle being probed, were:

- Regular Walk (RW) - *Gastrocnemius Medialis*;
- Calf Raise (CR) - *Gastrocnemius Medialis*;
- Wrist Flexion (WF) - *Flexor Carpi Radialis*;
- Wrist Extension (WE) - *Extensor Carpi Radialis Brevis*;

TABLE I
STATE OF THE ART COMPARISON AMONG sEMG ACTIVE PROBES

| **Reference** | Year | $A_{device}$ | $A_{electrode}$ | IED | Weight | Recording | Flexible | SNR[a] | Noise baseline | PC[b] |
|---|---|---|---|---|---|---|---|---|---|---|
| [15] | 2020 | 2115 $mm^2$ | 79 $mm^2$ | 20 mm | n.a. | Differential | ✓ | n.a. | n.a. | n.a. |
| [28] | 2020 | 1225 $mm^2$ | 510 $mm^2$ | n.a. | n.a. | Monopolar | ✓ | n.a. | 2 $mV_{peak\text{-}peak}$ | n.a. |
| [29] | 2020 | 1034 $mm^2$ | 64 $mm^2$ | 35 mm | n.a. | Differential | | 42.7 dB | n.a. | n.a. |
| [30] | 2021 | 99 $mm^2$ | 48 $mm^2$ | n.a. | n.a. | Monopolar | ✓[c] | n.a. | 2 $\mu V_{RMS}$ | 0.205 mW |
| [31] | 2023 | 1364 $mm^2$ | 225 $mm^2$ | 25 mm | 0.41 g | Differential | ✓ | 2.7 dB | n.a. | 1.45 mW |
| [32] | 2023 | n.a. | 16 $mm^2$ | 4 mm | n.a. | Differential | ✓ | 29.3 dB | 94 $\mu V_{RMS}$ | 1.25 mW |
| **This work** | 2024 | 251 $mm^2$ | 20 $mm^2$ | 20 mm | 0.81 g | Differential | ✓ | 10.9 dB | 78 $\mu V_{RMS}$ | 0.732 mW |

[a]Median value of the reported metric, [b]Power consumption, [c]Flexible and stretchable

- Jaw Closure (JC) - *Temporalis*;
- Shoulders Opening (SO) - *Trapezius Transversalis*.

The data were acquired at 1 kHz, by interfacing the DAQ with the MATLAB® software. The signals were then band-pass filtered at 20 Hz–400 Hz, rectified, and low-pass filtered again to obtain their envelopes. Then, the muscular rest and contraction phases were extracted based on envelope variations, excluding movement transients to ensure activation stability (see Fig. 2-b). From these windows, after bringing the signal back to its original dynamic (i.e., scaling the InAmp gain), three metrics were evaluated: Signal-to-Noise Ratio (SNR), Power Spectral Density (PSD), and baseline noise. For SNR evaluation, the standard deviations of the initial rest and of each contraction phase were computed, and the following formula was applied:

$$SNR = 10 \cdot \log_{10}\left(\frac{P_{\text{EMG}}}{P_{\text{noise}}}\right) = 10 \cdot \log_{10}\left(\frac{\sigma^2_{\text{signal}}}{\sigma^2_{\text{noise}}}\right)$$

Then, to ensure that no relevant variations in the frequency content occurred during dynamic exercises, a time-frequency analysis was conducted, with positive outcome. The PSDs of the contraction phases were thus estimated using the periodogram method with the Hamming window and then averaged to obtain a curve for each movement (Fig. 2-c).

Regarding the power consumption analysis, the Texas Instrument's (20 V/V gain) INA240 evaluation board was used. The output voltage of the board was then connected to an oscilloscope to display and save the acquired signal. The power consumption of the active probe was obtained by dividing the read voltages by 200 V/V · Ω (i.e., gain · $R_{\text{shunt}}$), to obtain the current values, which were then multiplied by the supply voltage (5 V provided by the DAQ) and averaged over time.

The obtained metrics are reported in Fig. 2. In particular, Fig. 2-b presents a typical raw signal, and the related envelope, acquired with the active probe, from which a baseline noise of around 78 $\mu V_{RMS}$ has been measured. This value can be improved by designing an acquisition board application-specific, thus ensuring a more stable acquisition setup. The PSDs shown in Fig. 2-c demonstrate that the active probe effectively records the typical frequencies of the sEMG spectrum [34]. The SNR computed for the six different movements, as shown in Fig. 2-d, exhibits a median value of 10.9 dB, indicating a good representation of muscle activity in dynamic movements, which generally yield lower values than controlled static contractions at high percentage of maximum voluntary contraction. Last, the power consumption was measured at 0.732 mW, a satisfactory value for utilizing the active probe on a battery-powered system suitable for long-term monitoring.

## IV. COMPARISON WITH SIMILAR WORKS

The proposed active probe is developed using dry-contact technology, also adopted by [15], [29], [30] with a gold-coated surface like [29]. In contrast, [28], [31], [32] incorporate capacitive electrodes. The implemented AFE includes an InAmp as [28], [29], [31] and an HPF like [15], [32], alongside a protection circuit as in [15]. Table I compares the mechanical and electrical performance of similar state of the art devices. Regarding SNR, among papers reporting values, the best performance was achieved by [29], albeit at the expense of larger sensor size and rigid support. In [30], a stretchable electrode was proposed, achieving significantly reduced baseline noise with compact dimensions and low power consumption. However, this setup requires separate placement of three monopolar electrodes and involves non-standardized manufacturing, comprising several processing phases. Among available commercial devices, Delsys offers the Trigno® Mini Sensor [35], which combines very compact size and high performance. However, these devices are made with rigid technology and are not open-source. All the above considered, the proposed active probe offers the smallest dimensions for differential sampling, very limited power consumption, and SNR and baseline noise performance comparable to state of the art works.

## V. CONCLUSIONS

A flexible dry-contact sEMG active probe has been proposed. This device, manufactured using rigid-flex PCB technology, enables differential measurement through gold-coated electrodes and on-board signal amplification and filtering stages. According to the tests conducted, the active probe achieved a good balance between mechanical and electrical performance. It features a compact size (30 mm x 10 mm x 3 mm), light weight (0.81 g), and low power consumption (0.732 mW). The quality of the acquired signals, with a median SNR of 10.9 dB and baseline noise of 78 µV during dynamic contractions, proves its applicability in muscle activity monitoring, minimizing discomfort for the subject.

## REFERENCES


[1] R. Merletti, A. Botter, and U. Barone, "Detection and conditioning of surface EMG signals," in *Surface Electromyography*, 1st ed., ser. IEEE Press Series on Biomedical Engineering. Hoboken, New Jersey: Wiley, 2016, pp. 1–37.

[2] M. Cavalcanti Garcia and T. M. Vieira, "Surface electromyography: Why, when and how to use it," *Revista Andaluza de Medicina del Deporte*, vol. 4, no. 1, pp. 17–28, 2011.

[3] M. Al-Ayyad, H. A. Owida, R. De Fazio, B. Al-Naami, and P. Visconti, "Electromyography monitoring systems in rehabilitation: A review of clinical applications, wearable devices and signal acquisition methodologies," *Electronics*, vol. 12, no. 7, 2023.

[4] F. Rossi, P. Motto Ros, R. M. Rosales, and D. Demarchi, "Embedded bio-mimetic system for functional electrical stimulation controlled by event-driven sEMG," *Sensors*, vol. 20, no. 5, p. 1535, Mar. 2020.

[5] Y. Zhou, Y. Fang, K. Gui, K. Li, D. Zhang, and H. Liu, "sEMG bias-driven functional electrical stimulation system for upper-limb stroke rehabilitation," *IEEE Sensors Journal*, vol. 18, no. 16, pp. 6812–6821, 2018.

[6] A. Fleming, N. Stafford, S. Huang, X. Hu, D. P. Ferris, and H. H. Huang, "Myoelectric control of robotic lower limb prostheses: A review of electromyography interfaces, control paradigms, challenges and future directions," *Journal of Neural Engineering*, vol. 18, no. 4, p. 041004, 2021.

[7] D. Leonardis, M. Barsotti, C. Loconsole, M. Solazzi, M. Troncossi, C. Mazzotti, V. P. Castelli, C. Procopio, G. Lamola, C. Chisari, M. Bergamasco, and A. Frisoli, "An EMG-controlled robotic hand exoskeleton for bilateral rehabilitation," *IEEE Transactions on Haptics*, vol. 8, no. 2, pp. 140–151, 2015.

[8] D. Shi, W. Zhang, W. Zhang, and et al., "A review on lower limb rehabilitation exoskeleton robots," *Chinese Journal of Mechanical Engineering*, vol. 32, p. 74, 2019.

[9] Q. Meng, J. Zhang, and X. Yang, "Virtual rehabilitation training system based on surface EMG feature extraction and analysis," *Journal of Medical Systems*, vol. 43, p. 48, 2019.

[10] A. Sturma, L. A. Hruby, C. Prahm, J. A. Mayer, and O. C. Aszmann, "Rehabilitation of upper extremity nerve injuries using surface EMG biofeedback: Protocols for clinical application," *Frontiers in Neuroscience*, vol. 12, p. 906, 2018.

[11] F. Rossi, F. Savi, A. Prestia, A. Mongardi, D. Demarchi, and G. Buccino, "Combining action observation treatment with a brain–computer interface system: Perspectives on neurorehabilitation," *Sensors*, vol. 21, no. 24, 2021. [Online]. Available: https://www.mdpi.com/1424-8220/21/24/8504

[12] A. Mongardi, F. Rossi, A. Prestia, P. Motto Ros, M. Ruo Roch, M. Martina, and D. Demarchi, "Hand gestures recognition for human-machine interfaces: A low-power bio-inspired armband," *IEEE Transactions on Biomedical Circuits and Systems*, vol. 16, no. 6, pp. 1348–1365, Dec. 2022.

[13] M. Zheng, M. S. Crouch, and M. S. Eggleston, "Surface electromyography as a natural human–machine interface: A review," *IEEE Sensors Journal*, vol. 22, no. 10, pp. 9198–9214, 2022.

[14] D. Farina, N. Jiang, H. Rehbaum, A. Holobar, B. Graimann, H. Dietl, and O. C. Aszmann, "The extraction of neural information from the surface EMG for the control of upper-limb prostheses: Emerging avenues and challenges," *IEEE Transactions on Neural Systems and Rehabilitation Engineering*, vol. 22, no. 4, pp. 797–809, 2014.

[15] A. M. Naim, K. Wickramasinghe, A. De Silva, M. V. Perera, T. D. Lalitharatne, and S. L. Kappel, "Low-cost active dry-contact surface EMG sensor for bionic arms," in *2020 IEEE International Conference on Systems, Man, and Cybernetics (SMC)*, 2020, pp. 3327–3332.

[16] A. D. Vigotsky, I. Halperin, G. J. Lehman, G. S. Trajano, and T. M. Vieira, "Interpreting signal amplitudes in surface electromyography studies in sport and rehabilitation sciences," *Frontiers in Physiology*, vol. 8, 2018.

[17] J. Taborri, J. Keogh, A. Kos, A. Santuz, A. Umek, C. Urbanczyk, E. van der Kruk, and S. Rossi, "Sport biomechanics applications using inertial, force, and EMG sensors: A literature overview," *Sport Biomechanics*, p. 2041549, 2020.

[18] P. Pakosz and M. Konieczny, "Training induced fatigability assessed by sEMG in pre-olympic ice-skaters," *Scientific Reports*, vol. 10, p. 14199, 2020.

[19] G. M. Hägg, A. Luttmann, and M. Jäger, "Methodologies for evaluating electromyographic field data in ergonomics," *Journal of Electromyography and Kinesiology*, vol. 10, pp. 301–312, 2000.

[20] S. E. Mudiyanselage, P. H. D. Nguyen, M. S. Rajabi, and R. Akhavian, "Automated workers' ergonomic risk assessment in manual material handling using sEMG wearable sensors and machine learning," *Electronics*, vol. 10, no. 20, 2021.

[21] A. Baraka, H. Shaban, M. Abou El-Nasr, and O. Attallah, "Wearable accelerometer and sEMG-based upper limb BSN for tele-rehabilitation," *Applied Sciences*, vol. 9, no. 14, 2019.

[22] C. M. Vidhya, Y. Maithani, and J. P. Singh, "Recent advances and challenges in textile electrodes for wearable biopotential signal monitoring: A comprehensive review," *Biosensors*, vol. 13, no. 7, p. 679, 2023.

[23] Y. Fu, J. Zhao, Y. Dong, and X. Wang, "Dry electrodes for human bioelectrical signal monitoring," *Sensors*, vol. 20, no. 13, p. 3651, 2020.

[24] Y. Jiang, O. W. Samuel, X. Liu, X. Wang, P. O. Idowu, P. Li, F. Chen, M. Zhu, Y. Geng, F. Wu, S. Chen, and G. Li, "Effective biopotential signal acquisition: Comparison of different shielded drive technologies," *Applied Sciences*, vol. 8, no. 2, p. 276, 2018.

[25] H. J. Hermens, B. Freriks, C. Disselhorst-Klug, and G. Rau, "Development of recommendations for sEMG sensors and sensor placement procedures," *Journal of Electromyography and Kinesiology*, vol. 10, no. 5, pp. 361–374, oct 2000.

[26] B. Afsharipour, S. Soedirdjo, and R. Merletti, "Two-dimensional surface EMG: The effects of electrode size, interelectrode distance and image truncation," *Biomedical Signal Processing and Control*, vol. 49, pp. 298–307, mar 2019.

[27] F. Rossi, A. Mongardi, P. Motto Ros, M. Ruo Roch, M. Martina, and D. Demarchi, "Tutorial: A versatile bio-inspired system for processing and transmission of muscular information," *IEEE Sensors Journal*, vol. 21, no. 20, pp. 22 285–22 303, 2021.

[28] C. L. Ng, M. B. I. Reaz, and M. E. H. Chowdhury, "A low noise capacitive electromyography monitoring system for remote healthcare applications," *IEEE Sensors Journal*, vol. 20, no. 6, pp. 3333–3342, 2020.

[29] J. A. Ruvalcaba, M. I. Gutiérrez, A. Vera, and L. Leija, "Wearable active electrode for sEMG monitoring using two-channel brass dry electrodes with reduced electronics," *Journal of Healthcare Engineering*, vol. 2020, pp. 1–11, 2020.

[30] Y. Jiang, L. Liu, L. Chen, Y. Zhang, Z. He, W. Zhang, J. Zhao, D. Lu, J. He, H. Zhu, Y. Gong, L.-R. Zheng, Y. Wang, Z. Li, and Y. Qin, "Flexible and stretchable dry active electrodes with PDMS and silver flakes for bio-potentials sensing systems," *IEEE Sensors Journal*, vol. 21, no. 10, pp. 12 255–12 268, 2021.

[31] C. L. Ng, M. B. I. Reaz, M. L. Crespo, A. Cicuttin, M. I. Bin Shapiai, S. H. Bin Md Ali, N. Binti Kamal, and M. E. H. Chowdhury, "A flexible capacitive electromyography biomedical sensor for wearable healthcare applications," *IEEE Transactions on Instrumentation and Measurement*, vol. 72, pp. 1–13, 2023.

[32] E. Genco, C. Garripoli, J.-L. P. J. Van Der Steen, G. H. Gelinck, S. Abdinia, P. Harpe, and E. Cantatore, "An EMG interface comprising a flexible A-IGZO active electrode matrix and a 65-nm CMOS IC," *IEEE Journal of Solid-State Circuits*, vol. 58, no. 11, pp. 3138–3149, November 2023.

[33] H. J. Hermens and B. Freriks, "Recommendations for sensor locations on individual muscles," https://www.seniam.org/, 2024, accessed: 2024-08-27.

[34] C. J. De Luca, *Surface Electromyography: Detection and Recording*. DelSys Incorporated, 2002.

[35] Delsys Inc., "Trigno mini," https://delsys.com/trigno-mini/, 2024, accessed: 2024-08-27.